IMPROVING DUAL-DOPPLER RETRIEVAL OF THE VERTICAL WIND USING A VERTICAL VORTICITY CONSTRAINT

Corey K. Potvin[1], Alan Shapiro[2,3], and Ming Xue[2,3]

[1]*NOAA National Severe Storms Laboratory, Norman, OK, USA, corey.potvin@noaa.gov*
[2]*School of Meteorology, University of Oklahoma, Norman, OK, USA*
[3]*Center for Analysis and Prediction of Storms, University of Oklahoma, Norman, OK, USA*

(Dated: 26 August 2011)

I. INTRODUCTION

The vertical velocity (w) is the most poorly-sampled wind component in typical (i.e., quasi-horizontal) radar scanning geometries. Dual-Doppler analyses of w are therefore largely dependent on the horizontal divergence term in the mass conservation constraint. Unfortunately, radial velocity data, and thus information about low-level divergence, are often lacking near the surface due to earth curvature, ground clutter and other factors. The resulting errors in the horizontal divergence estimated within the data gap can substantially degrade the analyzed w throughout the entire column.

A new mesoscale three-dimensional variational (3D-VAR) dual-Doppler analysis technique was developed by Shapiro et al. (2009), hereafter SPG09, that weakly (in a least-squares sense) satisfies the anelastic vertical vorticity equation in addition to the data constraint, a mass conservation equation and smoothness constraints. SPG09 showed that the vorticity equation can be used to improve retrievals of w when low-level radar data are lacking. The potential role of the vertical vorticity equation in improving mesoscale dual-Doppler retrievals of the 3D wind field has also been examined in Protat and Zawadzki (2000), Protat et al. (2001), Mewes and Shapiro (2002), and Liu et al. (2005).

In the present study, the impact of the vorticity constraint is further explored using an Advanced Regional Prediction System (ARPS; Xue et al. 2000, 2001) simulation of a supercell thunderstorm, as well as real Doppler observations of a tornadic supercell that occurred in Oklahoma on 8 May 2003. Several improvements to the original SPG09 technique are described and their impacts on the analyses examined. These modifications are primarily designed to better contend with unsteadiness in the observed flow.

II. MODIFIED COST FUNCTION

As in SPG09, the analyzed Cartesian wind components $u^a(x, y, z)$, $v^a(x, y, z)$ and $w^a(x, y, z)$ are obtained in this study by minimizing a cost function J that quantifies violations of data, mass conservation, vorticity and smoothness constraints. The relative impacts of each constraint on the analysis are controlled through weighting parameters, represented below by subscripted λ's. Also as in SPG09, estimates of the wind field translational velocity components U and V are used to mitigate errors in the data constraint due to observational nonsimultaneity and to improve the estimation of the local tendency term in the vorticity constaint. Unlike in SPG09, however, U and V are obtained in this study from a spatially-variable pattern-translation retrieval method (Shapiro et al. 2010a, b) rather than being assumed constant. This approach is better suited to the highly spatially-variable advection velocity fields typical of severe convective storms (e.g., left- and right-moving supercell pair). In addition, J is modified in some of our experiments to include pre-calculated estimates of the intrinsic evolution of the vertical vorticity field. These estimates are computed from provisional dual-Doppler analyses (with the vorticity constraint turned off) of two consecutive volume scans.

The data and mass conservation constraints are unchanged from SPG09. The smoothness cost function is modified in this study to use second-order rather than first-order spatial derivatives:

$$J_S \equiv \sum \lambda_S \left(\nabla^2 u^a + \nabla^2 v^a + \nabla^2 w^a \right).$$

The potential advantages and disadvantages of first- and second-order smoothing are discussed in SPG09. Although it is not clear *a priori* whether one option is generally preferable to the other, both produced similar RMS errors in our preliminary analyses (not shown).

The anelastic vertical vorticity equation used in the analysis procedure is

$$\frac{\partial \zeta}{\partial t} + \vec{u} \bullet \nabla \zeta + \left(\frac{\partial v}{\partial z}\frac{\partial w}{\partial x} - \frac{\partial u}{\partial z}\frac{\partial w}{\partial y} \right) + \zeta \left(\frac{\partial u}{\partial x} + \frac{\partial v}{\partial y} \right) = 0 ,$$

where the vertical vorticity $\zeta \equiv \partial v/\partial x - \partial u/\partial y$ and $\vec{u}$ is the 3-D wind vector. Justification for the use of this approximated vorticity equation is given in SPG09. For volume scan time intervals (hereafter, volume scan times) characteristic of current operational and research radars, we generally do not seek to compute the local vorticity derivative directly since this may introduce large temporal discretization errors. Instead, consider the total vorticity derivative in the reference frame following the wind field pattern:

$$\frac{D\zeta}{Dt} = \frac{\partial \zeta}{\partial t} + \vec{U} \bullet \nabla \zeta ,$$

where $\vec{U} \equiv U\hat{i} + V\hat{j}$ is the local horizontal advection velocity. Rearranging terms, we can write the local vorticity derivative as the sum of an intrinsic evolution term and a translation term:

$$\frac{\partial \zeta}{\partial t} = \frac{D\zeta}{Dt} - \vec{U} \bullet \nabla \zeta .$$

Substituting for the local derivative in our vorticity equation, we obtain:

$$\frac{D\zeta}{Dt}+\left(\vec{u}-\vec{U}\right)\cdot\nabla\zeta+\left(\frac{\partial v}{\partial z}\frac{\partial w}{\partial x}-\frac{\partial u}{\partial z}\frac{\partial w}{\partial y}\right)+\zeta\left(\frac{\partial u}{\partial x}+\frac{\partial v}{\partial y}\right)=0$$

In SPG09, only the contribution of the wind field translation to the local vorticity tendency was considered; that is, $D\zeta/Dt$ was implicitly set to zero. In the present study, however, we make provision for $D\zeta/Dt$. The new vorticity constraint can therefore be expressed as:

$$J_V \equiv \sum_{Cart}\lambda_V\left[\frac{D\zeta}{Dt}+(u^a-U)\frac{\partial\zeta^a}{\partial x}+(v^a-V)\frac{\partial\zeta^a}{\partial y}+w^a\frac{\partial\zeta^a}{\partial z}+\left(\frac{\partial v^a}{\partial z}\frac{\partial w^a}{\partial x}-\frac{\partial u^a}{\partial z}\frac{\partial w^a}{\partial y}\right)+\zeta^a\left(\frac{\partial u^a}{\partial x}+\frac{\partial v^a}{\partial y}\right)\right]^2.$$

III. EXPERIMENTS WITH ARPS SUPERCELL SIMULATION

The impact of the vorticity constraint was tested using a very high-resolution (Δx=Δy=25m) ARPS simulation of a supercell (Xue et al. 2007). This facilitated verification of analyses while providing a more realistic test of the technique than the analytical wind fields used in SPG09. The simulated storm exhibits many commonly-observed supercell features including a mesocyclone and associated strong central updraft, a hook-like signature in the emulated reflectivity field, and a rear-flank downdraft.

The dual-Doppler analyses proceeded over a 20 km × 20 km × 6 km subdomain (Δ = 500 m) of the ARPS simulation. Emulated radars positioned ~35 km from the center of the analysis domain scanned volume sectors that spanned ~90° in azimuth and elevation angles from 0.5° to 21.5°. Observations were computed from the model fields at range, azimuthal and elevational intervals of 200 m, 1° and 1°, respectively. The volume scan time T varied between our experiments from 30 s to 5 min, making the results relevant to dual-Doppler analyses of data from both rapidly-scanning radars such as the Doppler on Wheels (Wurman et al. 1997) and more conventional radars like the Weather Surveillance Radar 1988-Doppler (WSR-88D).

Three main types of retrievals were performed to explore the impact of the vorticity constraint: CONTROL, NOVORT and VORT. In all three retrieval types, the data, mass conservation and smoothness constraints were weakly imposed, and the impermeability condition was exactly satisfied at the ground. In the CONTROL experiments, all of the pseudo-observations were used. In the default NOVORT and VORT experiments, radial velocities lying below a data cutoff height z = 1.5 km were omitted from the retrievals. The vorticity constraint was weakly imposed in the VORT experiments only.

Including the vorticity constraint in the dual-Doppler analysis procedure reduced the RMS w^a error for all T (Fig. 1), with the greatest improvements occurring near the middle (z = 3 km) of the analysis domain. That the 5 min VORT retrieval was superior to the 30 s NOVORT retrieval highlights both the potentially significant impact of missing low-level data on vertical velocity analyses and the utility of the vorticity constraint in mitigating the resulting errors. Horizontal and vertical cross-sections of w^a reveal that the vorticity constraint produced the greatest improvement within the stronger updrafts (Fig. 2). The vorticity constraint had very little impact on u^a and v^a above the data void (not shown) since these are already well-determined by the remaining constraints.

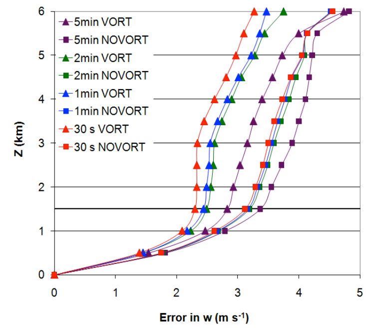

FIGURE 1: Impact of vorticity constraint for different T.

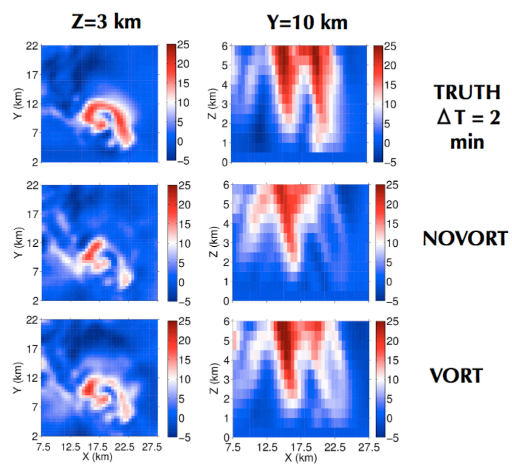

FIGURE 2: Horizontal (left) and vertical (right) cross-sections of true, NOVORT and VORT w.

Several variants of the VORT experiment were performed to examine the effects of accounting for the advection and evolution of the vorticity field: VORT-neither, VORT-adv and VORT-direct (Fig. 3). In the VORT-neither retrievals, the advection and evolution terms were set to zero, and so $\partial\zeta/\partial t$ = 0. In the VORT-adv retrievals, $D\zeta/Dt$ = 0. In the VORT-direct retrievals, $\partial\zeta/\partial t$ was calculated as an Eulerian derivative (i.e., in the fixed reference frame) from two provisional retrievals in which data advection correction was not used.

Setting $\partial\zeta/\partial t$ = 0 (VORT-neither) substantially diminished the utility of the vorticity constraint for all T. Not surprisingly, VORT-direct worked well for T = 30 s, but was disadvantageous for larger T due to increasing temporal discretization errors. The T = 5 min VORT-adv retrieval was actually slightly more accurate than the T = 5 min VORT retrieval. This is because the benefit of accounting for evolution (in addition to advection) of the vorticity field diminished with increasing T due to errors in the calculation of $D\zeta/Dt$. Thus, it may be prudent to set $D\zeta/Dt$ = 0 for very large T, though it should be noted that the value of T beyond which the evolution term becomes problematic may be highly case-dependent.

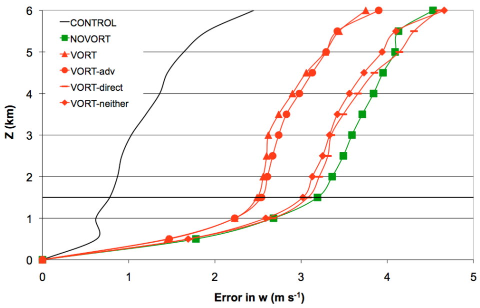

FIGURE 3: Impact of different methods for accounting for advection and evolution of vorticity (T = 2 min).

The VORT-adv retrievals were repeated using horizontally-uniform U, V fields in the data and vorticity constraints. The U, V were obtained for each T and analysis level by applying the iterative reflectivity-based Gal-Chen (1982) advection velocity retrieval method. The effect of using horizontally-uniform advection correction degraded the w^a by up to 6 %, 5 %, 2 % and 3 % for T = 30 s, 1 min, 2 min and 5 min, respectively. This confirmed the advantage of using spatially-variable advection correction.

IV. EXPERIMENTS WITH 8 MAY 2003 OKLAHOMA SUPERCELL RADAR DATA

The impact of the vorticity constraint was next explored using real Doppler radar observations of a tornadic supercell that passed over central Oklahoma on 8 May 2003. Data were collected by KTLX, a WSR-88D radar at Twin Lakes near Oklahoma City, and KOKC, a Terminal Doppler Weather Radar located ~25 km west-southwest of KTLX. The dual-Doppler analyses proceeded on a 20 km × 20 km × 3 km domain (Δ = 500 m). Since the true 3-D wind fields are not known, but high-quality radial wind data were available down to near the ground, we use the CONTROL analysis to verify the NOVORT and VORT retrievals.

Consistent with the ARPS experiments with the same volume scan time (T = 5 min), the w^a errors in VORT-adv were substantially reduced from both NOVORT and VORT-neither. The mesocyclonic updraft, the enhanced downdraft region located northwest of it, and the updraft atop the rear-flank gust front were all visibly better analyzed in VORT-adv than in NOVORT (Fig. 4).

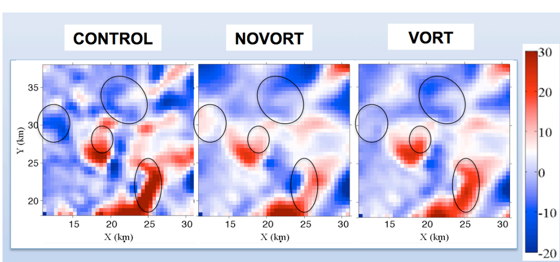

FIGURE 4: Impact of vorticity constraint in 8 May 2003 retrievals.

V. SUMMARY

We have demonstrated that imposing a vertical vorticity equation constraint can substantially improve dual-Doppler retrievals of w in supercell thunderstorms, especially when low-level radar coverage is lacking and volume scan times are short. Accounting for flow advection and evolution maximizes the utility of the vorticity constraint. Additional results are presented in Potvin et al. (2011).

VI. ACKNOWLEDGMENTS

This research was largely supported by the National Science Foundation (NSF) under Grant ATM-0532107. Part of the work was performed while the first author held a National Research Council Research Associateship Award at the National Severe Storms Laboratory (NSSL). Partial support of this work was provided by the NSSL. The authors were also supported by NSF grant EEC-0313747 and the third author also by NSF grants AGS-0802888, OCI-0905040, and AGS-0750790.

VII. REFERENCES

Liu, S., C. Qiu, Q. Xu, P. Zhang, J. Gao, and A. Shao, 2005: An improved method for Doppler wind and thermodynamic retrievals. *Adv. Atmos. Sci.*, **22**, 90–102.

Mewes, J. J., and A. Shapiro, 2002: Use of the vorticity equation in dual-Doppler analysis of the vertical velocity field. *J. Atmos. Oceanic Technol.*, **19**, 543–567.

Potvin, C. K., A. Shapiro, and M. Xue, 2011: Impact of a vertical vorticity constraint in variational dual-Doppler wind analysis: Tests with real and simulated supercell data. *J. Atmos. Oceanic Technol.*, accepted.

Protat, A., and I. Zawadzki, 2000: Optimization of dynamic retrievals from a multiple-Doppler radar network. *J. Atmos. Oceanic Technol.*, **17**, 753–760.

——, ——, and A. Caya, 2001: Kinematic and thermodynamic study of a shallow hailstorm sampled by the McGill bistatic multiple-Doppler radar network. *J. Atmos. Sci.*, **58**, 1222–1248.

Shapiro, A., C. K. Potvin, and J. Gao, 2009: Use of a vertical vorticity equation in variational dual-Doppler wind analysis. *J. Atmos. Oceanic Technol.*, **26**, 2089–2106.

——, K. M. Willingham, and C. K. Potvin, 2010: Spatially variable advection correction of radar data. Part I: Theoretical considerations. *J. Atmos. Sci*, **67**, 3445-3456.

——, ——, and ——, 2010: Spatially variable advection correction of radar data. Part II: Test results. *J. Atmos. Sci*, **67**, 3457-3470.

Wurman, J., J. Straka, E. Rasmussen, M. Randall, and A. Zahrai, 1997: Design and deployment of a portable, pencil-beam, pulsed, 3-cm Doppler radar. *J. Atmos. Oceanic Technol.*, **14**, 1502-1512.

Xue, M., K. K. Droegemeier, and V. Wong, 2000: The Advanced Regional Prediction System (ARPS)—A multiscale nonhydrostatic atmospheric simulation and prediction tool. Part I: Model dynamics and verification. *Meteor. Atmos. Phys.*, **75**:161–193.

——, and Coauthors, 2001: The Advanced Regional Prediction System (ARPS)—A multi-scale nonhydrostatic atmospheric simulation and prediction tool. Part II: Model physics and applications. *Meteor. Atmos. Phys.*, **76**, 143–165.

——, S. Liu, and T.-Y. Yu, 2007: Variational analysis of oversampled dual-Doppler radial velocity data and application to the analysis of tornado circulations. *J. Atmos. Oceanic Technol.*, **24**, 403–414.